RESEARCH ARTICLE

Modeling and Throughput Optimization of Multi-Gateway LoRaWAN

BAOGUO YU[1], **YACHUAN BAO**[1], **YUANKANG HUANG**[2], **WEN ZHAN**[2], (Member, IEEE),
AND **PEI LIU**[3,4,5], (Member, IEEE)

[1]State Key Laboratory of Satellite Navigation System and Equipment Technology, The 54th Research Institute of CETC, Shijiazhuang 050081, China
[2]School of Electronics and Communication Engineering, Sun Yat-sen University, Shenzhen 518107, China
[3]School of Information Engineering, Wuhan University of Technology, Wuhan 430070, China
[4]Key Lab of Broadband Wireless Communication and Sensor Network Technology (Nanjing University of Posts and Telecommunications), Ministry of Education, Nanjing 210003, China
[5]Integrated Computing and Chip Security Sichuan Collaborative Innovation Center of Chengdu University of Information Technology, Chengdu 610059, China

Corresponding authors: Wen Zhan (zhanw6@mail.sysu.edu.cn) and Pei Liu (pei.liu@ieee.org)

ABSTRACT Low power wide area network (LPWAN) technologies have become an integral part of Internet-of-Things (IoT) applications due to their ability to meet key requirements such as long range, low cost, massive device numbers, and low energy consumption. Among all available LPWAN technologies, LoRaWAN has garnered significant interest from both industry and academia. Due to wide communication range of LoRaWAN, the coverage of gateway (GW) may overlap and the packet transmissions from nodes in the overlapping area would collide, which deteriorates the network performance. How to tune the backoff parameter settings to reduce collision and maximize the network throughput in multi-GW LoRaWAN is still an open issue. To solve this issue, in this paper, we first propose a low-complexity model for multi-GW LoRaWAN, which divides nodes into different groups based on GWs they can communicate with. Key performance metrics, i.e., the network throughput, access delay and the probability of successful transmission, are derived as functions of backoff parameter and input rate. As the throughput performance crucially depends on whether each group is saturated or not, we propose an iterative algorithm to analyze the stability of the multi-GW LoRaWAN, based on which we further develop an iterative algorithm to tune the backoff parameter of each group iteratively for the network throughput optimization. The simulation results validate the effectiveness of the proposed algorithms and reveal the trade-off between fairness and efficiency.

INDEX TERMS LoRaWAN, multi-gateway network, throughput optimization, modeling, joint packet decoding, random access.

I. INTRODUCTION

Internet-of-Things (IoT) applications, such as smart agriculture and e-heath, have become increasingly pervasive, popular and crucial in human daily life. To ensure reliable links for IoT devices that may spread out in a large

The associate editor coordinating the review of this manuscript and approving it for publication was Renato Ferrero.

geographical area, wireless networks are required to provide robust operations and wide coverage with high energy efficiency and low cost. Regarding this, a new branch of IoT networking technology, called low power wide area networking (LPWAN), emerged and has attracted significant attention in recent years. Various LPWAN technologies were proposed, such as LTE-M, NB-IoT and LoRa. Among those promising solutions, LoRa has been the very popular one
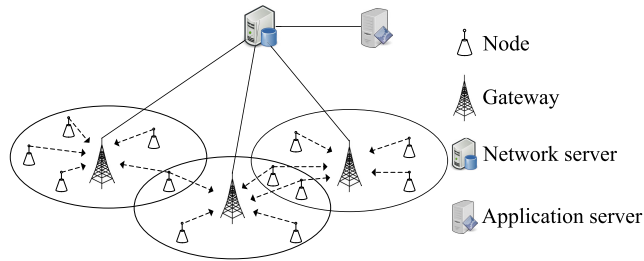
FIGURE 1. Network architecture of LoRaWAN.

due to its open-source attribute and scalability in network deployment that does not require telecom operators and licensed spectrum.

LoRa is a physical layer technology that defines a chirp spread spectrum (CSS) like modulation to enable long-range communication in the sub-Gigahertz unlicensed spectrum [1]. On the top of LoRa, LoRaWAN is the media access control (MAC) layer protocol that defines how IoT devices interact with each other [2]. As shown in Fig. 1, the topology of LoRaWAN is a star architecture, including nodes, gateways (GWs), network server (NS) and application server. In uplink communication, the nodes transmit packets to GWs, while GWs forward the packets to the NS. In general, there are multiple GWs in one LoRaWAN and the coverage area of GWs may overlap. The nodes located in the overlapping area can communicate with multiple GWs. It is different from traditional multi-cell networks [3], such as 5G, where *individual packet decoding* is used, i.e., each node is associated with a specific base station. In LoRaWAN, nodes are not associated with any specific gateway, such that each packet may be received by several GWs. The NS operates de-duplication to save the most reliable packet and discard the other copies [1]. In short, a packet can be successfully decoded if it is received by at least one GW. This characteristic is referred to as *joint packet decoding* in existing studies [4], [5], [6], [7], [8].

It should be pointed out that even with the joint packet decoding, the throughput performance of LoRaWAN couldn't be guaranteed. The reason stems from the random access scheme used in LoRaWAN. Specifically, with Aloha-type random access mechanism in LoRaWAN [9], each node independently determines when to access the channel and performs backoff once the transmission is failed. Aloha protocol is well known for its simplicity and ease of implementation, while it suffers from poor performance as torrents of channel access requests may burst in short period of time, leading to frequent packet collisions even multiple base stations collaboratively receive them. As the number of IoT devices and applications that LoRaWAN supports continues to grow, formulating a proper scheme to handle this challenge would be imperative to the success of the deployment of LoRaWAN in large-scale wide-area IoT scenario with massive machine-type communications (mMTC).

A. RELATED WORKS

There has been a long line of research on LoRaWAN, which starts with the single-GW case. Empirical results were presented in [10] to show the effect of system parameters, including spreading factor (SF), coding rate, payload size and packet generation interval, on the performance of LoRaWAN. In [11], decentralized dynamic SF allocation strategies based on deep reinforcement learning are proposed to improve network throughput and reduce energy consumption. With the stochastic geometry, [12], [13] revealed that the LoRaWAN performance decays exponentially with the number of nodes, indicating that interference among nodes, rather than noise, limits the network's performance in densely deployed networks. Reference [14] showed that the packet error rate increases with the network load in LoRaWAN and obtained the maximum network load that ensures reliable communication. Reference [15] analyzed the performance of LoRaWAN and revealed that to achieve a certain quantity of service (QoS) requirement in a single-GW LoRaWAN, the number of devices should be limited.

For the multi-GW scenario, SF allocation strategies to improve the performance of multi-GW LoRaWAN are proposed in [16] and [17]. Reference [16] proposed a spreading factor with priority (SF-P) algorithm for obtaining the optimal node distribution to improve the network throughput in multi-GW LoRaWAN including several IoT applications while respecting the priority requirements of different IoT applications. A SF allocation algorithm was proposed in [17] to enhance the packet delivery ratio (PDR) in both single-GW and multi-GW LoRaWAN as new devices progressively join the network. The allocation strategy is based on link PDR, network PDR, and network distribution of SF per gateway. References [18] and [19] studied the performance of multi-GW LoRaWAN under different conditions via simulators. Reference [18] presents a comparative performance analysis of multi-GW LoRaWAN in EU868 MHz spectrum and 2.4 GHz spectrum via simulator. Reference [19] compares the performance of adaptive strategies, namely the adaptive data rate (ADR) and the adaptive data payload (ADP) approaches, in dense scenarios featuring a variable number of gateways when network traffic is bidirectional. Reference [20] studied an algorithm to estimate the number of gateways to be activated according to the downlink traffic demand in the network, which is applicable to scenarios that the positions of nodes are unknown. Reference [1] and [21] studied how to improve the performance of multi-GW from the perspective of diversity. In [1], a novel cooperative decoding scheme was introduced based on GW diversity, which leverages multiple copies of the same packet received by different gateways to improve decoding reliability. Reference [21] proposed the use of spatial diversity in multi-GW LoRaWAN network, which can mitigate the path attenuation and make weak signals that may not be detectable can be successfully decoded. Reference [22] proposed a capture-based model for tuning inter-packet error correction codes (ECC) to achieve reliable communication.

References [23] and [24] used stochastic geometry tools to analyze the performance of multi-GW LoRaWAN by assuming the location distribution of nodes follows Poisson point process.

Most of above works for improving the performance of LoRaWAN focus on resource allocation, such as SF [11], [17]. While, scanty attention has been paid to the Aloha-type random access scheme in LoRaWAN. It has long been observed in existing literature on multi-cell Aloha network with individual packet decoding that the backoff parameters, such as the channel access probability, have significant influence on the throughput performance [25], [26]. It can be expected that in the multi-GW LoRaWAN with joint packet decoding, the backoff parameters should also be properly tuned for performance optimization. However, the optimal tuning of backoff parameters in LoRaWAN remains unknown. The challenge originates from two-fold: 1) Modeling methodology: Existing models on multi-GW LoRaWANs ignored the backoff behavior of each nodes and considered specific network topologies, such as Poisson point process [12], [13], [23], [24]. For general distribution of nodes, no suitable mathematical models for multi-GW LoRaWAN with joint packet decoding can capture the characteristics of device-level behavior. 2) Stability analysis: Existing research has revealed that the single-cell Aloha network has two steady-state points (i.e., the probability of successful transmissions of packets) and suffers the risk of dropping to the lower one, on which the network performance becomes poor [27]. The risk tightly relates to the system parameter settings, such as the traffic arrival rate and packet transmission probability. Characterizing the stable region in the single-cell Aloha networks is an non-trivial issue, which, as expected, will be more challenging in the multi-cell scenario.

B. OUR CONTRIBUTIONS
To address above open issues, this paper formulates a novel multi-group model for multi-GW LoRaWAN with joint packet decoding, investigates the bistable behavior of nodes and finally proposes an iterative algorithm on backoff parameter tuning for maximizing the throughput of multi-GW LoRaWAN. Our contributions are summarized as follow:

- By extending the analysis in [28], we develop a multi-group model for multi-GW LoRaWAN with joint packet decoding, in which each group corresponds to a set of nodes that can communicate with the same set of GWs. In contrast to the models in [12], [13], [23], and [24], the multi-group model does not limit to any specific geographic distribution of nodes. The behavior of head-of-line (HOL) packet of each node in each group is characterized and the steady-state probability of successful transmission is derived with the consideration of inter/intra group interference.
- By revisiting the stability analysis in the single-GW LoRaWAN, an iterative algorithm, which calculates the stable region and updates the saturation situation in each
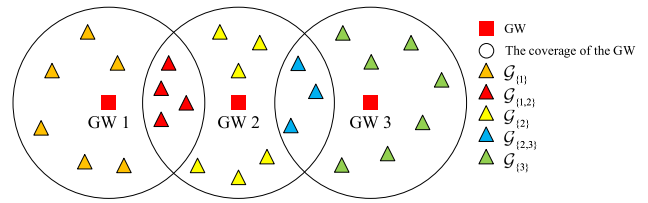

FIGURE 2. Graphic illustration of the nodes in different groups in a three GWs network.

iteration, is proposed for multi-GW LoRaWAN given the backoff parameter settings of all nodes. It is shown that in a saturated group, the backoff parameter is the predominant factor that determines group throughput, whereas in an unsaturated group, the packet arrival rate plays the key role.
- Both the throughput and delay performance are evaluated and an iterative algorithm is further proposed to optimize the network throughput, which tunes the backoff parameter setting of each group iteratively to maximize the number of unsaturated groups and use a convex optimization method to find the optimal backoff parameter settings of nodes in saturated groups. The proposed algorithm has low computational complexity and converges quickly, which indicates that the algorithm can be useful in practical multi-GW LoRaWANs.
- To facilitate the implementation of the proposed performance optimization scheme, we illustrate the signaling exchange procedure for the practical LoRaWAN based on specifications.

The outline of this paper is summarized as follow. Section II presents the system model. Section III analyzes the stability issue in multi-GW LoRaWAN and proposes an iterative algorithm to estimate the saturation situation of each group. Section IV develops the algorithm to optimize the throughput performance. Simulation results are presented in Section V to verify the analysis. The conclusion is given in Section VI.

II. SYSTEM MODEL AND PRELIMINARY ANALYSIS
A. SYSTEM MODEL
Consider a LoRaWAN with M GWs and n nodes. Let $\mathcal{M} = \{1, 2, .., M\}$ denote the set of GWs. Nodes located within the coverage area of GW i can communicate with GW i, $i \in \mathcal{M}$. As shown in Fig. 2, due to the wide-area coverage of LoRa GWs, a node might be covered by multiple GWs. Depending on different GWs each node can communicate with, we divide the nodes into different groups. Let $\mathcal{G}_{\mathcal{A}}$ denote the group of nodes which can be heard by all the GWs in set $\mathcal{A}$, with $|\mathcal{G}_{\mathcal{A}}| = n^{\mathcal{A}}$. Take red triangles in Fig. 2 for instance, they form the Group $\mathcal{G}_{\{1,2\}}$, which contains the nodes that can be heard by GW 1 and GW 2. As such, we have groups, $\mathcal{G}_{\{1\}}$, $\mathcal{G}_{\{2\}}$, $\mathcal{G}_{\{2,3\}}$ and $\mathcal{G}_{\{3\}}$.

Assume that packet arrivals at each node according to a Poisson process with rate λ (packets/second), and the buffer size of each node is infinite. According to
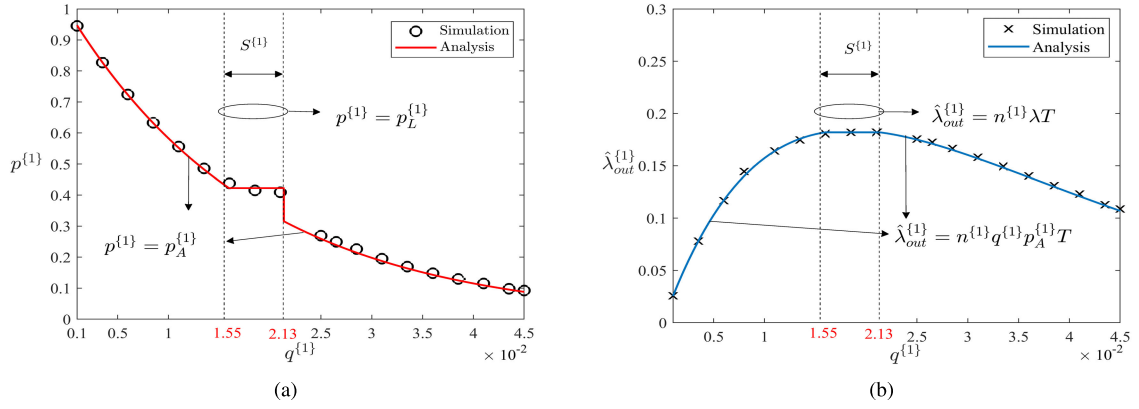
FIGURE 3. (a) Steady-state probability of successful transmission $p^{\{1\}}$ versus backoff parameter $q^{\{1\}}$. (b) Network throughput $\hat{\lambda}_{out}^{\{1\}}$ versus $q^{\{1\}}$. $M = 1$, $\lambda = 6.74 \times 10^{-3}$ (packets/second), $T = 0.45$ (second), $n^{\{1\}} = 60$.

LoRaWAN specification [9], LoRaWAN provides 8 channels and 6 SFs for nodes and the packets with different SF are quasi-orthogonal to each other [10]. The LoRa symbol time length is $T = \frac{2^{SF}}{BW}$ (second) [1], where BW denotes the bandwidth of the channel, SF denotes the spreading factor of the node. In this paper, the classical collision model is considered, that is, a packet transmitted in time t can be successfully received by a GW in time $t + T$ if and only if no other packets with the same SF are transmitted to the GW through the same channel during interval $(t - T, t + T)$. We assume all nodes use the same SF and share a common channel, because nodes with different SF and channels would not collide with each other. Each node in $\mathcal{G}_{\mathcal{A}}$, which involves in a collision, performs backoff with the length of backoff interval following the exponential distribution with parameter $q^{\mathcal{A}1}$. To simplify the analysis, we consider delay first transmission, that is, a new HOL packet executes backoff before its first transmission.

In LoRaWAN, GWs forward the successfully received packets to the NS. The GW is transparent to the nodes, which are connected to the NS [8]. The NS operates deduplication to save the most reliable packet and discard the other copies. Therefore, we can regard the joint packet decoding is used in LoRaWANs, i.e., a packet can be successfully decoded if it is successfully received by at least one GW. The ACK/NACK transmission from the GW is instantaneous and error-free. For each GW, it can be regarded a pure Aloha system with each packet lasting for T seconds, for which let us first revisit the stability analysis of single-cell pure Aloha system in the next subsection.

B. STABILITY ANALYSIS IN SINGLE GW SCENARIO

Consider a single-GW LoRaWAN network with $n^{\{1\}}$ nodes belonging to Group $\mathcal{G}_{\{1\}}$. We denote the steady state

---

[1] According to LoRa specification [9], the time length of each backoff is an non-linear increasing function of the number of collisions that the node experiences. We adopt the exponential backoff to approximate the backoff process to ease the analysis, similar to [29], and the analysis can be readily extended to the scenario where other backoff schemes are used.

probability of successful transmission of Group $\mathcal{G}_{\{1\}}$ as $p^{\{1\}}$. According to [30], $p^{\{1\}}q^{\{1\}}$ and λ are the service rate and the input rate of each data queue, respectively. The offered load $\rho^{\{1\}}$ of each data queue can be written as

$$\rho^{\{1\}} = \begin{cases} \frac{\lambda}{p^{\{1\}}q^{\{1\}}} < 1 & \text{Group } \mathcal{G}_{\{1\}} \text{ is unsaturated,} \\ 1 & \text{Group } \mathcal{G}_{\{1\}} \text{ is saturated.} \end{cases} \quad (1)$$

In the saturated case, each node always has packets to transmit and $\rho^{\{1\}} = 1$. For a HOL packet, it can be successfully received if and only if other $n^{\{1\}} - 1$ nodes don't request transmission within interval $(t - T, t + T)$, with probability $(\Pr\{X > 2T\})^{n^{\{1\}}-1}$, where

$$\Pr\{X > 2T\} = \int_{2T}^{+\infty} q^{\{1\}} \exp\{-q^{\{1\}}x\}dx$$
$$= \exp\{-2q^{\{1\}}T\}, \quad (2)$$

and X denotes the backoff interval length of an arbitrary node. Accordingly, the probability of successful transmission in saturated situation, $p_A^{\{1\}}$, can be obtained as

$$p_A^{\{1\}} = (\Pr\{X > 2T\})^{n^{\{1\}}-1} \approx \exp\{-2n^{\{1\}}q^{\{1\}}T\}, \quad (3)$$

by approximating $n^{\{1\}} - 1 \approx n^{\{1\}}$.

In the unsaturated case, the data queues of nodes may be empty with probability $\rho^{\{1\}} < 1$. The probability that a node has packets to transmit during $(t - T, t + T)$ is $2T\rho^{\{1\}}$, based on which a node does not request transmission within $(t - T, t + T)$ is given by $\Pr\{X > 2T\rho^{\{1\}}\}$. By further combining (2), we can obtain

$$p^{\{1\}} = (\Pr\{X > 2T\rho^{\{1\}}\})^{n^{\{1\}}-1}$$
$$\approx \exp\{-2n^{\{1\}}q^{\{1\}}T\rho^{\{1\}}\}, \quad (4)$$

which has two non-zero roots

$$\begin{cases} p_L^{\{1\}} = \exp\{\mathbb{W}_0(-2n^{\{1\}}\lambda T)\} \\ p_S^{\{1\}} = \exp\{\mathbb{W}_{-1}(-2n^{\{1\}}\lambda T)\} \end{cases}, \quad (5)$$

when $n^{\{1\}}\lambda T \leq \frac{1}{2}e^{-1}$. $\mathbb{W}_0(\cdot)$ and $\mathbb{W}_{-1}(\cdot)$ denote the two branches of the Lambert W function [31].

Define the group throughput as the number of successful transmission per T seconds and denote the group throughput of group $\mathcal{G}_\mathcal{A}$ as $\hat{\lambda}_{out}^\mathcal{A}$. In single GW scenario, the group throughput can be expressed as [30]

$$\hat{\lambda}_{out}^{\{1\}} = \begin{cases} n^{\{1\}}\lambda T & \text{Group } \mathcal{G}_{\{1\}} \text{ is unsaturated,} \\ n^{\{1\}}q^{\{1\}}Tp_A^{\{1\}} & \text{otherwise.} \end{cases} \quad (6)$$

In terms of backoff parameter $q^{\{1\}}$, the stable region of Group $\mathcal{G}_{\{1\}}$ can be defined as

$$S^{\{1\}} \triangleq \left\{ q^{\{1\}} | \hat{\lambda}_{out}^{\{1\}} = n^{\{1\}}\lambda T \right\}. \quad (7)$$

The following theorem presents the explicit expression of $S^{\{1\}}$.

Theorem 1. *The stable region in the single GW scenario can be expressed as*

$$S^{\{1\}} = \left[-\frac{\mathbb{W}_0(-2n^{\{1\}}\lambda T)}{2n^{\{1\}}T}, -\frac{\mathbb{W}_{-1}(-2n^{\{1\}}\lambda T)}{2n^{\{1\}}T} \right], \quad (8)$$

when $n^{\{1\}}\lambda T \leq \frac{1}{2e}$.

    Proof: See Appendix A. ∎

The above analysis is verified via simulations. We developed a MATLAB-based simulator. Each simulation runs 10^8 slots and each time slot represents 0.01 seconds. The probability of successful transmission probability of each group is obtained by calculating the ratio of the number of successful packets to the number of transmission packets. The throughput of each group is obtained by calculating the ratio of the number of successful packets to the number of symbol time $\frac{2 \times 10^6}{T}$. We can clearly see from Fig.3 (a) and (b) that the group is unsaturated when $q^{\{1\}} \in S^{\{1\}}$, the probability of successful transmission $p^{\{1\}} = p_L^{\{1\}}$ is independent of the backoff parameter $q^{\{1\}}$ according to (5) and the group throughput $\hat{\lambda}_{out}^{\{1\}}$ is maximized at $n^{\{1\}}\lambda T$. Otherwise, the probability of successful transmission $p^{\{1\}} = p_A^{\{1\}}$ declines with $q^{\{1\}}$ and the throughput performance degrades.

III. STABILITY ANALYSIS IN MULTI-GW LORAWAN NETWORKS

We can see that in the single-GW case, the throughput performance crucially depends on whether the group is saturated or not. It can be expected that in the multi-GW scenario, i.e., $M > 1$, determining whether each group is saturated or not is also an issue of crucial importance, which is the focus of this section.

A. STEADY-STATE POINT OF EACH GROUP

Assume the saturation condition of each group is known, for which we let saturation indicator to represent

$$\Delta^\mathcal{A} \triangleq \begin{cases} 0 & \text{Group } \mathcal{G}_\mathcal{A} \text{ is unsaturated,} \\ 1 & \text{Group } \mathcal{G}_\mathcal{A} \text{ is saturated,} \end{cases} \quad (9)$$

for $\mathcal{A} \subset \mathcal{M}$. Denote the probability of successful transmission of group $\mathcal{G}_\mathcal{A}$ as $p^\mathcal{A}$ and we will derive $p^\mathcal{A}$ given $\Delta^\mathcal{A}$.

Consider a HOL packet from Group $\mathcal{G}_\mathcal{A}$ transmitted in time t. With joint packet decoding among GWs, the packet can be successfully decoded if and only if two conditions hold: 1) other nodes in Group $\mathcal{G}_\mathcal{A}$ don't transmit during $(t - T, t + T)$, 2) at least one of the GWs in set $\mathcal{A}$ doesn't receive other packets during $(t - T, t + T)$. Then, we can express the steady-state probability that the HOL packet can be successfully transmitted as

$$p^\mathcal{A} \approx \Pr\{\text{Node in Group } \mathcal{G}_\mathcal{A} \text{ with no request}\}^{n^\mathcal{A}} \left(1 - \prod_{j \in \mathcal{A}} \right.$$

$$\left. (1 - \prod_{\substack{\mathcal{D}=\tilde{\mathcal{D}} \cup \{j\} \\ \tilde{\mathcal{D}} \subset \mathcal{M}\backslash\{j\} \\ \mathcal{D} \neq \mathcal{A}}} \Pr\{\text{Node in Group } \mathcal{G}_\mathcal{D} \text{ with no request}\}^{n^\mathcal{D}}) \right). \quad (10)$$

According to the analysis in Section II, the probability that nodes in an unsaturated group $\mathcal{G}_\mathcal{A}$ don't transmit packet during $(t - T, t + T)$ is $\exp\left\{ -\frac{2n^\mathcal{A}\lambda T}{p^\mathcal{A}} \right\}$. The probability that nodes in a saturated group $\mathcal{G}_\mathcal{A}$ don't transmit packet during $(t - T, t + T)$ is $\exp\{-2n^\mathcal{A}q^\mathcal{A}T\}$. Accordingly, when Group $\mathcal{G}_\mathcal{A}$ is unsaturated, (10) can be rewritten as

$$p^\mathcal{A} = \exp\left\{ -\frac{2n^\mathcal{A}\lambda T}{p^\mathcal{A}} \right\} \left(1 - \prod_{j \in \mathcal{A}} R_j \right). \quad (11)$$

R_j denotes the interference from other groups located in the coverage of GW j, with

$$R_j = 1 - \exp\left\{ \sum_{\substack{\mathcal{D}=\tilde{\mathcal{D}} \cup \{j\} \\ \tilde{\mathcal{D}} \subset \mathcal{M}\backslash\{j\} \\ \mathcal{D} \neq \mathcal{A} \\ \Delta^\mathcal{D}=0}} -\frac{2n^\mathcal{D}\lambda T}{p^\mathcal{D}} - \sum_{\substack{\mathcal{D}=\tilde{\mathcal{D}} \cup \{j\} \\ \tilde{\mathcal{D}} \subset \mathcal{M}\backslash\{j\} \\ \mathcal{D} \neq \mathcal{A} \\ \Delta^\mathcal{D}=1}} 2n^\mathcal{D}q^\mathcal{D}T \right\} \quad (12)$$

When Group $\mathcal{G}_\mathcal{A}$ is saturated, (10) can be rewritten as

$$p^\mathcal{A} = \exp\left\{ -2n^\mathcal{A}q^\mathcal{A}T \right\} \left(1 - \prod_{j \in \mathcal{A}} R_j \right). \quad (13)$$

We can see from (11) and (13) that the transmission of a HOL packet from Group $\mathcal{G}_\mathcal{A}$ is interfered by other nodes in Group $\mathcal{G}_\mathcal{A}$ and the nodes in neighboring groups located within the coverage of GWs in set $\mathcal{A}$. To derive the steady-state points according to (11) and (13), the saturation indicator of each group $\Delta^\mathcal{D}, \mathcal{D} \subset \mathcal{M}$, should be given. How to determine the saturation situation of each group will be the key focus of the following subsection.

B. STABILITY ANALYSIS IN THE MULTI-GW SCENARIO

It has long been known that determining the saturation condition of nodes in random access networks is a challenging problem. Due to the coupling effect among the groups, the expressions of stable regions in the multi-GW scenario are extremely difficult, if not impossible, to be explicitly

---

Algorithm 1 Iterative Algorithm for Obtaining $\{\Delta^{\mathcal{A}}, \mathcal{A} \subset \mathcal{M}\}$

1: Initialize $\{\Delta_0^{\mathcal{A}}, \mathcal{A} \subset \mathcal{M}\}$ according to (14) and (15).
2: **repeat**
3:      Based on $\{\Delta_{k-1}^{\mathcal{A}}, \mathcal{A} \subset \mathcal{M}\}$, obtain $\{p_k^{\mathcal{A}}, \mathcal{A} \subset \mathcal{M}\}$ from (11) and (13).
4:      **for** $\mathcal{A} \subset \mathcal{M}$ **do**
5:          **if** $\Delta_{k-1}^{\mathcal{A}} = 0$ and $S_k^{\mathcal{A}}$ exists **then**
6:              Obtain $S_k^{\mathcal{A}}$ from (16).
7:              Update $\Delta_k^{\mathcal{A}}$ according to (17).
8:          **end if**
9:      **end for**
10: **until** $\{\Delta_k^{\mathcal{A}}, \mathcal{A} \subset \mathcal{M}\} = \{\Delta_{k-1}^{\mathcal{A}}, \mathcal{A} \subset \mathcal{M}\}$
11: $\{\Delta^{\mathcal{A}}, \mathcal{A} \subset \mathcal{M}\} \leftarrow \{\Delta_k^{\mathcal{A}}, \mathcal{A} \subset \mathcal{M}\}$.
12: $\{S^{\mathcal{A}}, \mathcal{A} \subset \mathcal{M}\} \leftarrow \{S_k^{\mathcal{A}}, \mathcal{A} \subset \mathcal{M}\}$.
13: **Output:** $\{\Delta^{\mathcal{A}}, \mathcal{A} \subset \mathcal{M}\}$ and $\{S^{\mathcal{A}}, \mathcal{A} \subset \mathcal{M}\}$

Algorithm 2 Algorithm for Obtaining $\{q^{\mathcal{A},*}, \mathcal{A} \subset \mathcal{M}\}$

1: **Initialization:** $q_0^{\mathcal{A}} \leftarrow \frac{1}{2n^{\mathcal{A}}T}$, for $\mathcal{A} \subset \mathcal{M}$. $k = 0$.
2: Execute Algorithm 1 to obtain $\{S^{\mathcal{A}}, \mathcal{A} \subset \mathcal{M}\}$.
3: **repeat**
4:      $k \leftarrow k + 1$.
5:      **for** $\mathcal{A} \subset \mathcal{M}$ **do**
6:          **if** $S^{\mathcal{A}} \neq \varnothing$ **then**
7:              $q_k^{\mathcal{A}} \leftarrow q_l^{\mathcal{A}}$.
8:          **else if** $S^{\mathcal{A}} = \varnothing$ **then**
9:              Obtain the root of (21), q_{root}.
10:              $q_k^{\mathcal{A}} = \max\{0, q_{root}\}$.
11:          **end if**
12:      **end for**
13: **until** $\{q_k^{\mathcal{A}}, \mathcal{A} \subset \mathcal{M}\} = \{q_{k-1}^{\mathcal{A}}, \mathcal{A} \subset \mathcal{M}\}$
14: $\{q^{\mathcal{A},*}, \mathcal{A} \subset \mathcal{M}\} \leftarrow \{q_k^{\mathcal{A}}, \mathcal{A} \subset \mathcal{M}\}$
15: **Output:** $\{q^{\mathcal{A},*}, \mathcal{A} \subset \mathcal{M}\}$.

---

characterized. Accordingly, we propose an iterative algorithm (i.e., Algorithm 1) based on the stable region of each group in Theorem 1 to obtain the saturation indicators in the multi-GW scenario.

Specifically, in the initial step of the algorithm, we ignore the interference from other groups and treat each group as a single-GW LoRaWAN to calculate the stable region of each group if it exists, which can be denoted as

$$S_0^{\mathcal{A}} = \left[-\frac{\mathbb{W}_0(-2n^{\mathcal{A}}\lambda T)}{2n^{\mathcal{A}}T}, -\frac{\mathbb{W}_{-1}(-2n^{\mathcal{A}}\lambda T)}{2n^{\mathcal{A}}T} \right], \quad (14)$$

for $\mathcal{A} \subset \mathcal{M}$. $S_0^{\mathcal{A}}$ exists if and only if $2n^{\mathcal{A}}\lambda T < \exp\{-1\}$. Then the saturation indicator in the initial step can be expressed as

$$\Delta_0^{\mathcal{A}} = \begin{cases} 0 & q^{\mathcal{A}} \in S_0^{\mathcal{A}}, \\ 1 & \text{else}, \end{cases} \quad (15)$$

for $\mathcal{A} \subset \mathcal{M}$. In each iteration, we calculate the steady-state probability of successful transmission of each group based on the saturation indicators calculated in the last iteration to obtain new saturation indicators. For example, in k^{th} iteration, we calculate $\{p_k^{\mathcal{A}}, \mathcal{A} \subset \mathcal{M}\}$ from (11) and (13), by assuming the saturation indicators are given by $\{\Delta_{k-1}^{\mathcal{A}}, \mathcal{A} \subset \mathcal{M}\}$. If $\Delta_{k-1}^{\mathcal{A}} = 0$ and $S_k^{\mathcal{A}}$ exists, we calculate $S_k^{\mathcal{A}}$ from

$$S_k^{\mathcal{A}} = \left[-\frac{\mathbb{W}_0\left(-\frac{2n^{\mathcal{A}}\lambda T}{1-\prod\limits_{j\in\mathcal{A}} R_{j,k}}\right)}{2n^{\mathcal{A}}T}, -\frac{\mathbb{W}_{-1}\left(-\frac{2n^{\mathcal{A}}\lambda T}{1-\prod\limits_{j\in\mathcal{A}} R_{j,k}}\right)}{2n^{\mathcal{A}}T} \right], \quad (16)$$

where $R_{j,k}$ is the interference from groups located within the coverage area of GW j calculated at k^{th} iteration, which can be obtained from (12). Appendix B gives the proof of (16). $S_k^{\mathcal{A}}$ can be regarded as the stable region calculated with the consideration of interference from other groups and it exists

FIGURE 4. Number of iterations k of Algorithm 2 versus M with different input rate λ. $T = 0.5$(second), $n^{\{i\}} = 50$, $n^{\{i,j\}} = 25$, $i, j \in \mathcal{M}$, $i \neq j$.

if and only if $\frac{2n^{\mathcal{A}}\lambda T}{1-\prod\limits_{j\in\mathcal{A}} R_{j,k}} < \exp\{-1\}$. Based on (16) we update the saturation indicator according to

$$\Delta_k^{\mathcal{A}} = \begin{cases} 0 & q^{\mathcal{A}} \in S_k^{\mathcal{A}}, \\ 1 & \text{else}. \end{cases} \quad (17)$$

Then repeat the loop, until the saturation indicators are converged, i.e, $\Delta_k^{\mathcal{A}} = \Delta_{k-1}^{\mathcal{A}}$, for $\mathcal{A} \subset \mathcal{M}$. The details of the proposed iterative algorithm are in Algorithm 1.

IV. THROUGHPUT OPTIMIZATION IN MULTI-GWS LORAWAN

This section aims at optimizing the throughput performance of the multi-GW LoRaWAN by tuning the backoff parameter setting of each group. The group throughput of Group $\mathcal{G}_{\mathcal{A}}$ can be written as

$$\hat{\lambda}_{out}^{\mathcal{A}} = \begin{cases} n^{\mathcal{A}}\lambda T & \Delta^{\mathcal{A}} = 0, \\ n^{\mathcal{A}}q^{\mathcal{A}}p^{\mathcal{A}}T & \Delta^{\mathcal{A}} = 1, \end{cases} \quad (18)$$
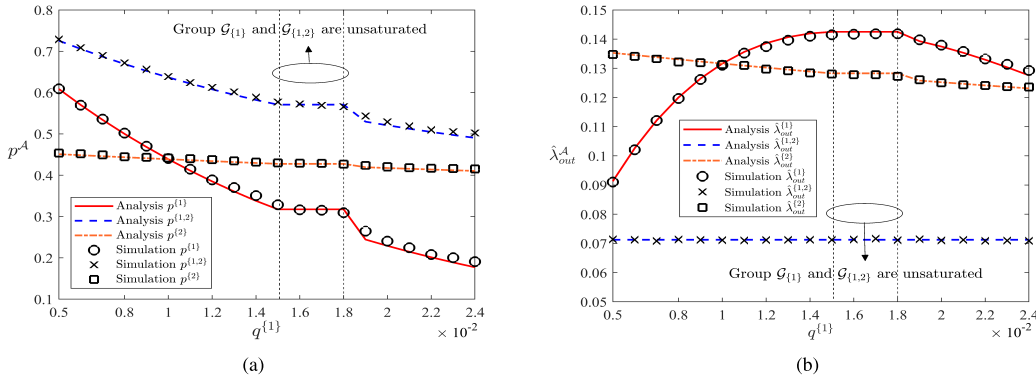
FIGURE 5. $M = 2$, $T = 0.5$ (second), $n^{\{1\}} = n^{\{2\}} = 60$, $n^{\{1,2\}} = 30$, $q^{\{1,2\}} = q^{\{2\}} = 1 \times 10^{-3}$, $\lambda = 4.75 \times 10^{-3}$ (packets/second). (a) Successful transmission probability of each group versus $q^{\{1\}}$. (b) Throughput of each group versus $q^{\{1\}}$.

according to (6). The network throughput is defined as the sum of the throughput of all groups and can be expressed as

$$\hat{\lambda}_{out} = \sum_{\mathcal{A} \subset \mathcal{M}} \hat{\lambda}_{out}^{\mathcal{A}}. \qquad (19)$$

Accordingly, the optimization problem can be formulated as

$$\hat{\lambda}_{max} = \max_{\substack{0 \le q^{\mathcal{A}} \le 1, \\ \mathcal{A} \subset \mathcal{M}}} \hat{\lambda}_{out}. \qquad (20)$$

Due to the coupling effect among the groups, solving the above problem is challenging. Recall from Algorithm 1 that adjusting the backoff parameter of one group may change the saturation conditions of many other groups, which further changes the expressions of the group throughput according to (18). Regarding this, based on Algorithm 1, we further propose another iterative algorithm, Algorithm 2, to obtain the optimal backoff parameter settings $\{q^{\mathcal{A},*}, \mathcal{S} \subset \mathcal{M}\}$ for network throughput maximization. The basic idea of the Algorithm 2 is illustrated below.

In the initialization step of Algorithm 2, the backoff parameter of each group is set to be $\frac{1}{2n^{\mathcal{A}}T}$, i.e, the root of $\frac{\partial \hat{\lambda}_{out}^{\mathcal{A}}}{\partial q^{\mathcal{A}}} = 0$ given Group $\mathcal{G}_{\mathcal{A}}$ is saturated. Then in step 6 to 7, we tune $q^{\mathcal{A}}$ to be the lower bound of the stable region calculated at $k-1^{\text{th}}$ iteration, with $q_l^{\mathcal{A}} = -\dfrac{\mathbb{W}_0\left(-\frac{2n^{\mathcal{A}}\lambda T}{1 - \prod_{j \in \mathcal{A}} R_{j,k}}\right)}{2n^{\mathcal{A}}T}$, when $S^{\mathcal{A}}$ exists, because the lower bound is the least value that can ensure Group $\mathcal{G}_{\mathcal{A}}$ stay unsaturated while reduce the channel contention to the greatest extent. In step 8 to 9, we tune the transmission probability of the groups with $S^{\mathcal{A}} = \varnothing$ to be the root of $\frac{\partial \hat{\lambda}_{out}}{\partial q^{\mathcal{A}}} = 0$ in (21) if it is positive.

$$\frac{\partial \hat{\lambda}_{out}}{\partial q^{\mathcal{A}}} = n^{\mathcal{A}} p^{\mathcal{A}} T (1 - 2n^{\mathcal{A}} T q^{\mathcal{A}}) + \sum_{\substack{\phi \subset \mathcal{M} \\ \phi \cap \mathcal{A} \ne \varnothing \\ \Delta^{\mathcal{A}} = 1 \\ \phi \ne \mathcal{A}}} n^{\phi} q^{\phi} T$$

$$\exp\{-2n^{\phi} q^{\phi} T\} \left(1 - \prod_{j \in (\phi \cap \mathcal{A})} \left(1 + 2n^{\mathcal{A}} T \prod_{\substack{\mathcal{D} = \tilde{\mathcal{D}} \cup \{j\} \\ \tilde{\mathcal{D}} \subset \mathcal{M} \setminus \{j\} \\ \Delta^{\mathcal{A}} = 0}}\right.\right.$$

$$\left.\left.\exp\{-\frac{2n^{\mathcal{D}} \lambda T}{p^{\mathcal{D}}}\} \prod_{\substack{\mathcal{D} = \tilde{\mathcal{D}} \cup \{j\} \\ \tilde{\mathcal{D}} \subset \mathcal{M} \setminus \{j\} \\ \Delta^{\mathcal{A}} = 1}} \exp\{-2n^{\mathcal{D}} q^{\mathcal{D}} T\}\right) \prod_{\substack{j \notin (\phi \cap \mathcal{A}) \\ j \in \phi}} R_j\right). \qquad (21)$$

Repeat the loop until the backoff parameter of each group converges.

To evaluate the convergence speed of Algorithm 2, let us consider one representative multi-GW topology illustrated in Fig. 2, where GWs are placed in a linear manner. Fig. 4 presents the number of iterations of Algorithm 2 in terms of the number of GWs M. When $\lambda = 2 \times 10^{-3}$, k is always equal to 2, indicating that Algorithm 2 converges immediately when the input rate is low. For this case, the stable region of each group exists, i.e, $\frac{2n^{\mathcal{A}}\lambda T}{1 - \prod_{j \in \mathcal{A}} R_{j,k}} < \exp\{-1\}$. Therefore, Algorithm 2 effectively adjusts the backoff parameter configurations of each group to the lower bound of their stable region, resulting in rapid convergence. This process is demonstrated explicitly in steps 6 to 7 of Algorithm 2. With a larger input rate, there may exist groups for which the stable regions don't exist. To optimize these groups, a convex optimization technique is employed, which is depicted in step 8 to 11 of Algorithm 2 and incurs higher computational overhead. Thus we can see from Fig. 4 that k gradually increases as M increases and eventually reaches a state of equilibrium when λ is 6×10^{-3} or 7×10^{-3}. Fig. 4 illustrates that the value of k consistently stays below 10, revealing the swift convergence speed of Algorithm 2 for arbitrary input rate and network scale. This characteristic satisfies the demands of practical applications.

V. SIMULATIONS AND IMPLEMENTATION ON MULTI-GW LORAWAN THROUGHPUT OPTIMIZATION
This section investigates the effectiveness of the proposed algorithms and further demonstrates how the algorithms can be implemented to practical multi-GW LoRaWAN.

A. SIMULATION RESULTS
The simulation settings are consistent with that in Section II-B, except that the number of GWs $M > 1$.
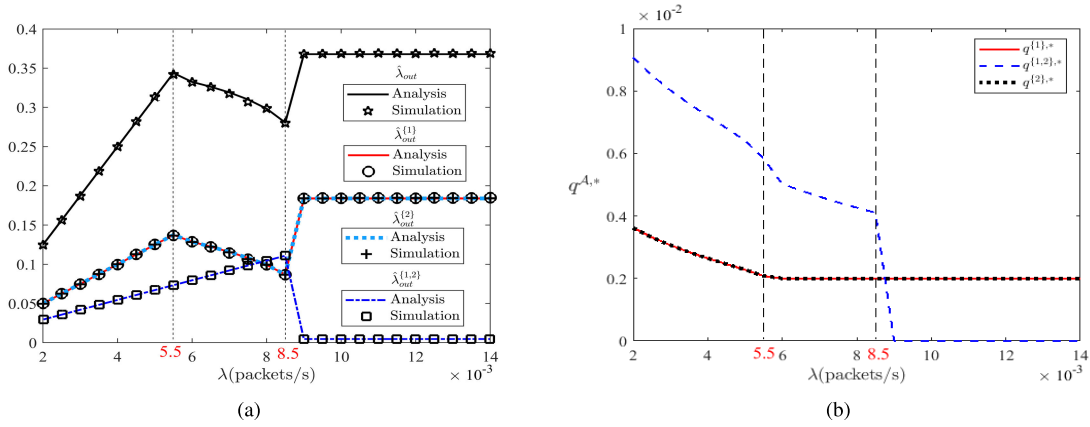
FIGURE 6. $M = 2$, $T = 0.5$ (second), $n^{\{1\}} = n^{\{2\}} = 50$, $n^{\{1,2\}} = 25$. (a) Network throughput $\hat{\lambda}_{out}$ and the throughput of each group versus input rate λ. (b) The optimal backoff parameter setting of each group versus input rate λ.

In our simulations, GWs are placed in a linear manner as illustrated in Fig. 2. Fig. 5 demonstrates how the successful transmission probability and throughput of each group vary with the backoff parameter of group $\mathcal{G}_{\{1\}}$ with $M = 2$ and $q^{\{1,2\}} = q^{\{2\}} = 1 \times 10^{-3}$. It shows that Algorithm 1 can correctly determine the saturation situation of each group. Specifically, we observe that when $q^{\{1\}}$ increases from 5×10^{-3} to 1.5×10^{-2}, Group $\mathcal{G}_{\{1\}}$ and $\mathcal{G}_{\{2\}}$ stay saturated, while Group $\mathcal{G}_{\{1,2\}}$ is always unsaturated. When $q^{\{1\}}$ increases from 1.5×10^{-2} to 1.8×10^{-2}, all groups becomes unsaturated and the successful transmission probability stays unchanged, while the throughput of Group $\mathcal{G}_{\{1\}}$ and $\mathcal{G}_{\{1,2\}}$ is equal to the aggregate input rate, which is the maximum value. When $q^{\{1\}}$ further increases, Group $\mathcal{G}_{\{1\}}$ and $\mathcal{G}_{\{2\}}$ become saturated again. As $q^{\{1\}}$ increases, Group $\mathcal{G}_{\{1\}}$ produces more transmission requests and thus, $p^{\{1\}}$ and $p^{\{1,2\}}$ decrease. Due to the coupling effect network-wide, $p^{\{2\}}$ also decreases, although the decreasing rate is small.

Fig. 6a demonstrates the network throughput and group throughput in terms of the input rate, where the back-off parameter settings of groups are tuned according to Algorithm 2 and shown in Fig. 6b. When λ increases from 2×10^{-3} to 5.5×10^{-3}, the network throughput and the throughput of each group grow linearly because the input rate is small and all groups are unsaturated. We can conclude that when input rate is small, Algorithm 2 can ensure all groups are unsaturated and maximize the network throughput. When λ is greater than 8.5×10^{-3}, the throughput and the backoff parameter of Group $\mathcal{G}_{\{1,2\}}$ decrease sharply to 0 which indicates that the nodes located in the overlapping coverage area should be muted to maximize the network throughput when input rate is large. In this case, we can conclude that with Algorithm 2, although the network throughput performance is optimized, the group throughput is sacrificed. The fairness issue arises and could be an interesting topic that deserves much attention in future work.
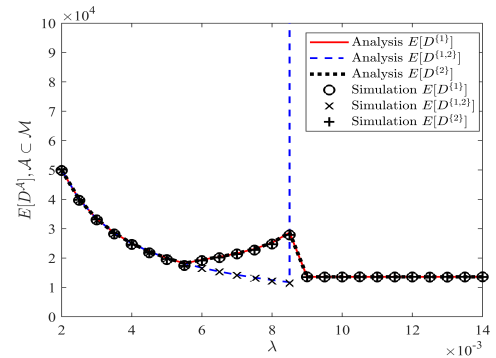

FIGURE 7. $M = 2$, $T = 0.5$ (second), $n^{\{1\}} = n^{\{2\}} = 50$, $n^{\{1,2\}} = 25$. The mean access delay versus input rate λ.

B. DISCUSSION ON ACCESS DELAY IN MULTI-GW LORAWAN

In this subsection, we further analyze the delay performance of multi-GW LoRaWAN. In this paper, we define access delay as the service time of HOL packets. Denote the access delay of Group $\mathcal{G}_{\mathcal{A}}$ as $D^{\mathcal{A}}$. As is mentioned in Section II-B, the service rate of Group $\mathcal{G}_{\mathcal{A}}$ is $p^{\mathcal{A}} q^{\mathcal{A}}$. So we can obtain the mean access delay of Group $\mathcal{G}_{\mathcal{A}}$ as

$$E[D^{\mathcal{A}}] = \frac{1}{p^{\mathcal{A}} q^{\mathcal{A}}}. \tag{22}$$

Fig. 7 demonstrates the mean access delay of each group in terms of input rate, where the backoff parameter settings are tuned according to Algorithm 2. When λ increases from 2×10^{-3} to 5.5×10^{-3}, the mean access delay is the same for all groups, because all groups are unsaturated. However, when λ is greater than 8.5×10^{-3}, $E[D^{\{1,2\}}]$ is infinite, indicating that to optimize the network throughput, nodes located in the overlapping area would experience infinite access delay when the input rate is large.

C. IMPLEMENTATION ON LORAWAN

The analysis presented in this paper sheds important light on the practical multi-GW LoRaWAN design as LoRaWAN
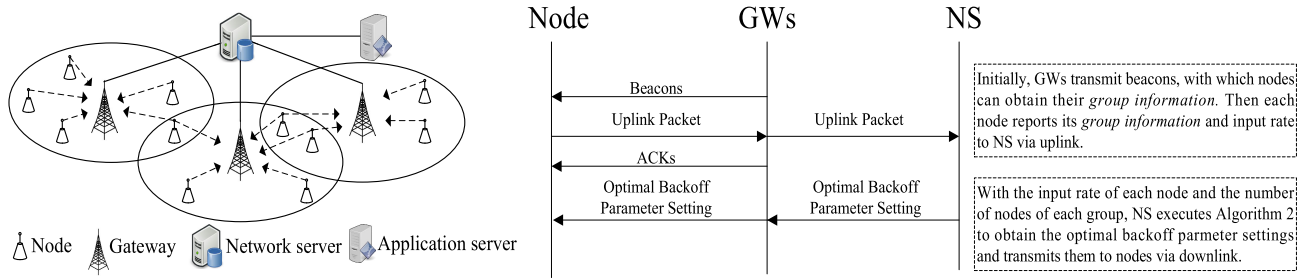
FIGURE 8. Implementation of algorithm 2 in practical LoRaWAN.

specification does not provide instructions on how to configure the backoff parameter. To optimize the throughput performance, the backoff parameter of each group need to be adaptively tuned according to the number of nodes of each group and the input rate λ. The optimal backoff parameter can be obtained from Algorithm 2 with fast convergence speed. According to the LoRaWAN specification [9], there are three types of devices in LoRaWAN, including Class A, Class B, Class C. Class A operating mode has two downlink receive windows following each uplink transmission window. Class B mode opens additional receive windows at specific time scheduled by gateways through beacons. Class C mode always opens receive windows. As the difference between the three types of devices lies only in the downlink receive window, this paper only discusses how to implement throughput optimization in LoRaWAN with Class B devices.

Fig. 8 illustrates how to implement Algorithm 2 in practical LoRaWAN. Initially, the input rate of each node and the number of nodes in each group are unknown to NS, which are necessary for executing Algorithm 2. So GWs broadcast beacons with which nodes can obtain their *group information*, i.e., the information indicating which group the node belongs to[2]. Then each node reports its *group information* and input rate to NS via uplink packet. Given the number of nodes in each group and the input rate of each node, NS operates Algorithm 2 to obtain the optimal backoff parameter settings and transmits them to nodes via downlink. When either the number of nodes or the input rate of each node changes, NS can recalculate the optimal settings, and broadcast them again. We can see that only the signaling overhead of beacons are introduced for implementing the optimal configuration. The main overhead of implementation may come from Algorithm 2. We can see from Fig.4 that the convergence speed of Algorithm 2 is fast, so Algorithm 2 would not be computationally expensive and time-consuming. Therefore, the analytical results in this paper are promising to be used in practical networks.

---

[2]According to LoRa specification [9], each beacon consists of preamble, network common part and gateway-specific part. By demodulating the gateway-specific part of beacon, the node can detect the ID of the GW and obtain its *group information*.

VI. CONCLUSION
This paper focus on modeling and throughput optimization of multi-GW LoRaWAN with joint packet decoding. The analysis starts with a multi-group model for characterizing the geographic relationship among nodes and GWs. This model is applicable to arbitrary location distributions of nodes and enables the derivation of key performance metrics, such as steady-state probability of successful transmission and network/group throughput. Based on the queueing behavior characterization of each node in each group, we propose an iterative algorithm that can determine the saturation situation of each group given the backoff parameters of nodes. As the backoff parameter can be tuned, we further propose an iterative algorithm for the network throughput performance optimization. The proposed schemes are verified by a MATLAB-based simulator and simulation results show that our algorithm can achieve nearly optimal network throughput, i.e, $\frac{M}{2} \exp\{-1\}$, under different traffic scenarios. The analysis shows that there exist the coupling effect among the groups in multi-GW LoRaWAN, that is, the transmission of nodes may not only affect the other nodes in the same group, but also influence neighboring groups. With a large input rate, the nodes located in the overlapping coverage area must be muted to maximized the network throughput, indicating the trade-off between fairness and efficiency. The fairness issue could be an interesting topic that deserves much attention in our future work.

APPENDIX A
DERIVATION OF THE STABLE REGION IN (8)
The stable region $S^{\{1\}}$ of Group $\mathcal{G}_{\{1\}}$ can be divided into 2 parts, i.e, $S^{\{1\}} = S_L^{\{1\}} \cup S_A^{\{1\}}$, where $S_L^{\{1\}}$ denotes the stable region when the group is unsaturated and $S_A^{\{1\}}$ denotes the stable region when the group is saturated. According to [27], [32], the group is unsaturated if two conditions hold: 1) the offered load, $\rho^{\{1\}}$, is no greater than 1, i.e, $\rho^{\{1\}} = \frac{\lambda}{p_L^{\{1\}} q^{\{1\}}} \leq 1$, 2) the transient probability of successful transmission $p_t^{\{1\}}$ stays greater than $p_S^{\{1\}}$. The lower bound of stable region $q_l^{\{1\}}$ can be obtained from the first condition as

$$q_l^{\{1\}} = \frac{\lambda}{p_L^{\{1\}}} = -\frac{\mathbb{W}_0(-2n^{\{1\}}\lambda T)}{2n^{\{1\}}T}. \tag{23}$$

Consider a HOL packet transmitted in time $t - T$ and assume that there are n_b nodes with non-empty data queue during $(t - 2T, t)$. The transient probability that the HOL packet can be successfully received in time t can be expressed as $p_t^{\{1\}} = \exp\{-2n_b q^{\{1\}} T\}$. If $q^{\{1\}} \leq \lambda$, $p_t^{\{1\}} \geq \exp\{-2n^{\{1\}} q^{\{1\}} T\} \geq \exp\{-2n^{\{1\}} \lambda T\}$. According to (76) in [27], $2n^{(\{1\})} \lambda T < -\mathbb{W}_{-1}(-2n^{\{1\}} \lambda T) = -\ln p_S^{(\{1\})}$. So $p_t^{\{1\}}$ is greater than $p_S^{\{1\}}$ if $q^{\{1\}} \leq \lambda < -\frac{\ln p_S^{\{1\}}}{2n^{\{1\}} T}$. If $q^{\{1\}} > \lambda$, $p_t^{\{1\}} \geq \exp\{-2n^{\{1\}} q^{\{1\}} T\}$. Obviously, $p_t^{\{1\}}$ is no less than $p_S^{\{1\}}$ if $\lambda < q^{\{1\}} \leq -\frac{\ln p_S^{\{1\}}}{2n^{\{1\}} T}$. So $q_u^{\{1\}}$ can be obtained as

$$q_u^{\{1\}} = -\frac{\ln p_S^{\{1\}}}{2n^{\{1\}} T} = -\frac{\mathbb{W}_{-1}(-2n^{\{1\}} \lambda T)}{2n^{\{1\}} T}. \qquad (24)$$

Then consider the network is saturated. In this situation, the throughput is determined by the aggregate service rate per symbol time and is not smaller than the aggregate input rate per symbol time, i.e, $\hat{\lambda}_{out}^{\{1\}} = n^{\{1\}} q^{\{1\}} p_A^{\{1\}} T \geq n^{\{1\}} \lambda T$. Obviously, $n^{\{1\}} q^{\{1\}} p_A^{\{1\}} T$ is lower than $n^{\{1\}} \lambda T$ when $q^{\{1\}} > q_u^{\{1\}}$ or $q^{\{1\}} < q_l^{\{1\}}$. So $S_A^{\{1\}}$ doesn't exist and $S^{\{1\}} = S_L^{\{1\}} = [q_l^{\{1\}}, q_u^{\{1\}}]$.

APPENDIX B
DERIVATION OF THE STABLE REGION IN (16)

Consider Group $\mathcal{G}_\mathcal{A}$ with $\Delta_{k-1}^\mathcal{A} = 0$. According to (11), we can obtain the equation of $p_k^\mathcal{A}$, which denotes the probability of success of Group $\mathcal{G}_\mathcal{A}$ in k^{th} epoch as

$$p_k^\mathcal{A} = \exp\{-\frac{2n^\mathcal{A} \lambda T}{p^\mathcal{A}}\}\left(1 - \prod_{j \in \mathcal{A}} R_{j,k}\right), \qquad (25)$$

where $R_{j,k}$ denotes the interference from groups located within the coverage area of GW j calculated at k^{th} iteration, with

$$R_{j,k} = 1 - \exp\{\sum_{\substack{\mathcal{D}=\tilde{\mathcal{D}} \cup \{j\} \\ \tilde{\mathcal{D}} \subset \mathcal{M}\backslash\{j\} \\ \mathcal{D} \neq \mathcal{A} \\ \Delta_{k-1}^\mathcal{D}=0}} -\frac{2n^\mathcal{D} \lambda T}{p^\mathcal{D}} - \sum_{\substack{\mathcal{D}=\tilde{\mathcal{D}} \cup \{j\} \\ \tilde{\mathcal{D}} \subset \mathcal{M}\backslash\{j\} \\ \mathcal{D} \neq \mathcal{A} \\ \Delta_{k-1}^\mathcal{D}=1}} -2n^\mathcal{D} q^\mathcal{D} T\}. \qquad (26)$$

Equation (25) has two non-zero roots

$$p_{L,k}^\mathcal{A} = -\frac{2n^\mathcal{A} \lambda T}{\mathbb{W}_0(-\frac{2n^\mathcal{A} \lambda T}{1 - \prod_{j \in \mathcal{A}} R_{j,k}})}, \qquad (27)$$

and

$$p_{S,k}^\mathcal{A} = -\frac{2n^\mathcal{A} \lambda T}{\mathbb{W}_{-1}(-\frac{2n^\mathcal{A} \lambda T}{1 - \prod_{j \in \mathcal{A}} R_{j,k}})}, \qquad (28)$$

when $\frac{2n^\mathcal{A} \lambda T}{1 - \prod_{j \in \mathcal{A}} R_{j,k}} \leq \frac{1}{e}$. The group is unsaturated if two conditions hold: 1) the offered load, $\rho^\mathcal{A}$, is no greater than 1, 2) the transient probability of successful transmission $p_t^\mathcal{A}$ stay

greater than $p_{S,k}^\mathcal{A}$. From condition 1, we can obtain the lower bound of $S_k^\mathcal{A}$ as

$$q_{l,k}^\mathcal{A} = \frac{\lambda}{p_{L,k}^\mathcal{A}} = -\frac{\mathbb{W}_0\left(-\frac{2n^\mathcal{A} \lambda T}{1 - \prod_{j \in \mathcal{S}} R_{j,k}}\right)}{2n^\mathcal{A} T}. \qquad (29)$$

Consider a HOL packet from Group $\mathcal{G}_\mathcal{A}$ transmitted in time $t - T$ and assume that there are n_b nodes with non-empty data queue in Group $\mathcal{G}_\mathcal{A}$ during $(t - 2T, t)$. The transient probability that the HOL packet can be successfully received in time t can be expressed as

$$p_t^\mathcal{A} = \exp\{-2n_b q^\mathcal{A} T\}\left(1 - \prod_{j \in \mathcal{A}} R_{j,k}\right). \qquad (30)$$

If $q^\mathcal{A} \leq \lambda$, $p_t^\mathcal{A} \geq \exp\{-2n^\mathcal{A} q^\mathcal{A} T\} \geq \exp\{-2n^\mathcal{A} \lambda T\}$. According to (76) in [27], $2n^\mathcal{A} \lambda T < -\mathbb{W}_{-1}(-2n^\mathcal{A} \lambda T) \leq \mathbb{W}_{-1}(-\frac{2n^\mathcal{A} \lambda T}{1 - \prod_{j \in \mathcal{A}} R_{j,k}})$. So $p_t^\mathcal{A}$ is greater than $p_{S,k}^\mathcal{A}$ if $q^\mathcal{A} \leq \lambda < -\frac{\mathbb{W}_{-1}\left(-\frac{2n^\mathcal{A} \lambda T}{1 - \prod_{j \in \mathcal{S}} R_{j,k}}\right)}{2n^\mathcal{A} T}$. If $q^\mathcal{A} > \lambda$, $p_t^{\{1\}} \geq \exp\{-2n^{\{1\}} q^{\{1\}} T\}$. Obviously, $p_t^\mathcal{A}$ is no less than $p_S^\mathcal{A}$ if $\lambda < q^\mathcal{A} \leq -\frac{\mathbb{W}_{-1}\left(-\frac{2n^\mathcal{A} \lambda T}{1 - \prod_{j \in \mathcal{S}} R_{j,k}}\right)}{2n^\mathcal{A} T}$. So the upper bound $q_{u,k}^\mathcal{A}$ can be obtained as

$$q_{u,k}^\mathcal{A} = -\frac{\mathbb{W}_{-1}\left(-\frac{2n^\mathcal{A} \lambda T}{1 - \prod_{j \in \mathcal{S}} R_{j,k}}\right)}{2n^\mathcal{A} T}. \qquad (31)$$

REFERENCES

[1] A. Petroni and M. Biagi, "Interference mitigation and decoding through gateway diversity in LoRaWAN," *IEEE Trans. Wireless Commun.*, vol. 21, no. 11, pp. 9068–9081, Nov. 2022.

[2] J. P. S. Sundaram, W. Du, and Z. Zhao, "A survey on LoRa networking: Research problems, current solutions, and open issues," *IEEE Commun. Surveys Tuts.*, vol. 22, no. 1, pp. 371–388, 1st Quart., 2020.

[3] J. Ding, D. Qu, P. Liu, and J. Choi, "Machine learning enabled preamble collision resolution in distributed massive MIMO," *IEEE Trans. Commun.*, vol. 69, no. 4, pp. 2317–2330, Apr. 2021.

[4] S. Ogata, K. Ishibashi, and G. T. F. de Abreu, "Optimized frameless ALOHA for cooperative base stations with overlapped coverage areas," *IEEE Trans. Wireless Commun.*, vol. 17, no. 11, pp. 7486–7499, Nov. 2018.

[5] D. Jakovetic, D. Bajovic, D. Vukobratovic, and V. Crnojevic, "Cooperative slotted ALOHA for multi-base station systems," *IEEE Trans. Commun.*, vol. 63, no. 4, pp. 1443–1456, Apr. 2015.

[6] C.-H. Yu, L. Huang, C.-S. Chang, and D.-S. Lee, "Poisson receivers: A probabilistic framework for analyzing coded random access," *IEEE/ACM Trans. Netw.*, vol. 29, no. 2, pp. 862–875, Apr. 2021.

[7] R. Wang, P. Li, G. Cui, W. Wang, and Y. Zhang, "Cooperative slotted ALOHA with reservation for multi-receiver satellite IoT networks," in *Proc. IEEE/CIC Int. Conf. Commun. China (ICCC)*, Aug. 2018, pp. 593–597.

[8] A. Mastilovic, D. Vukobratovic, D. Jakovetic, and D. Bajovic, "Cooperative slotted ALOHA for massive M2M random access using directional antennas," in *Proc. IEEE Int. Conf. Commun. Workshops (ICC Workshops)*, May 2017, pp. 731–736.

[9] *LoRaWAN Specification v1.1*, LoRa Alliance Technical Committee, San Francisco, CA, USA, 2017.

[10] Md. R. Islam, M. Bokhtiar-Al-Zami, B. Paul, R. Palit, J.-C. Grégoire, and S. Islam, "Interference issues in LoRaWAN: A comparative study using simulator and analytical model," in *Proc. IEEE Region 10th Symp. (TENSYMP)*, Jul. 2022, pp. 1–6.

[11] M. Chen, L. Mokdad, J. Ben-Othman, and J.-M. Fourneau, "Dynamic parameter allocation with reinforcement learning for LoRaWAN," *IEEE Internet Things J.*, vol. 10, no. 12, pp. 10250–10265, Jun. 2023.

[12] O. Georgiou and U. Raza, "Low power wide area network analysis: Can LoRa scale?" *IEEE Wireless Commun. Lett.*, vol. 6, no. 2, pp. 162–165, Apr. 2017.

[13] A. Mahmood, E. Sisinni, L. Guntupalli, R. Rondón, S. A. Hassan, and M. Gidlund, "Scalability analysis of a LoRa network under imperfect orthogonality," *IEEE Trans. Ind. Informat.*, vol. 15, no. 3, pp. 1425–1436, Mar. 2019.

[14] D. Bankov, E. Khorov, and A. Lyakhov, "Mathematical model of LoRaWAN channel access with capture effect," in *Proc. IEEE 28th Annu. Int. Symp. Pers., Indoor, Mobile Radio Commun. (PIMRC)*, Oct. 2017, pp. 1–5.

[15] I. E. Korbi, Y. Ghamri-Doudane, and L. A. Saidane, "LoRaWAN analysis under unsaturated traffic, orthogonal and non-orthogonal spreading factor conditions," in *Proc. IEEE 17th Int. Symp. Netw. Comput. Appl. (NCA)*, Nov. 2018, pp. 1–9.

[16] A. Loubany, S. Lahoud, A. E. Samhat, and M. E. Helou, "Throughput improvement for LoRaWAN networks considering IoT applications priority," in *Proc. 6th Conf. Cloud Internet Things (CIoT)*, Mar. 2023, pp. 206–210.

[17] M. N. Ochoa, M. Maman, and A. Duda, "Spreading factor allocation for LoRa nodes progressively joining a multi-gateway adaptive network," in *Proc. IEEE Global Commun. Conf. (GLOBECOM)*, Dec. 2020, pp. 1–6.

[18] R. Marini and G. Cuozzo, "A comparative performance analysis of LoRaWAN in two frequency spectra: EU868 MHz and 2.4 GHz," in *Proc. Joint Eur. Conf. Netw. Commun. 6G Summit (EuCNC/6G Summit)*, Jun. 2023, pp. 1–6.

[19] E. Sisinni, A. Depari, P. Bellagente, A. Flammini, I. Silva, T. Flores, and P. Ferrari, "Can adaptive strategies sustain bidirectional LoRaWAN traffic?" in *Proc. IEEE Int. Workshop Metrology Ind. 4.0 IoT (MetroInd4.0 IoT)*, Jun. 2023, pp. 66–71.

[20] S. Javed and D. Zorbas, "Downlink traffic demand-based gateway activation in LoRaWAN," in *Proc. IEEE Symp. Comput. Commun. (ISCC)*, Jul. 2023, pp. 669–674.

[21] A. Dongare, R. Narayanan, A. Gadre, A. Luong, A. Balanuta, S. Kumar, B. Iannucci, and A. Rowe, "Charm: Exploiting geographical diversity through coherent combining in low-power wide-area networks," in *Proc. 17th ACM/IEEE Int. Conf. Inf. Process. Sensor Netw. (IPSN)*, Apr. 2018, pp. 60–71.

[22] M. Heusse, C. Caillouet, and A. Duda, "Performance of unslotted ALOHA with capture and multiple collisions in LoRaWAN," *IEEE Internet Things J.*, vol. 10, no. 20, pp. 17824–17838, Oct. 2023.

[23] O. Georgiou, C. Psomas, and I. Krikidis, "Coverage scalability analysis of multi-cell LoRa networks," in *Proc. IEEE Int. Conf. Commun. (ICC)*, Jun. 2020, pp. 1–7.

[24] Y. Bouazizi, F. Benkhelifa, and J. McCann, "Spatiotemporal modelling of multi-gateway LoRa networks with imperfect SF orthogonality," in *Proc. IEEE Global Commun. Conf. (GLOBECOM)*, Dec. 2020, pp. 1–7.

[25] A. S. Galanopoulos and R. L. Hamilton, "Recursive retransmission control for a two-station slotted-ALOHA network," *IEEE Trans. Commun.*, vol. 42, no. 234, pp. 1722–1728, Feb. 1994.

[26] Y. Yang and L. Dai, "Stability region and transmission control of multi-cell ALOHA networks," *IEEE Trans. Commun.*, vol. 71, no. 9, pp. 5348–5364. Sep. 2023.

[27] L. Dai, "Stability and delay analysis of buffered Aloha networks," *IEEE Trans. Wireless Commun.*, vol. 11, no. 8, pp. 2707–2719, Aug. 2012.

[28] Y. Gao, L. Dai, and X. Hei, "Throughput optimization of multi-BSS IEEE 802.11 networks with universal frequency reuse," *IEEE Trans. Commun.*, vol. 65, no. 8, pp. 3399–3414, Aug. 2017.

[29] J.-B. Seo, B. C. Jung, and H. Jin, "Modeling and online adaptation of ALOHA for low-power wide-area networks (LPWANs)," *IEEE Internet Things J.*, vol. 8, no. 20, pp. 15608–15619, Oct. 2021.

[30] D. Gross, J. F. Shortle, J. M. Thompson, and C. M. Harris, *Fundamentals of Queueing Theory*, 4th ed. Hoboken, NJ, USA: Wiley, 2008.

[31] R. M. Corless, G. H. Gonnet, D. E. G. Hare, D. J. Jeffrey, and D. E. Knuth, "On the Lambert W function," *Adv. Comput. Math.*, vol. 5, no. 1, pp. 329–359, 1996.

[32] W. Zhan and L. Dai, "Massive random access of machine-to-machine communications in LTE networks: Modeling and throughput optimization," *IEEE Trans. Wireless Commun.*, vol. 17, no. 4, pp. 2771–2785, Apr. 2018.

BAOGUO YU is currently the Director of CEPNT, the Chief Scientist of The 54th Research Institute of CETC, a member of the National BD Standardization Technical Committee and the Technology Committee of the National Administration of Surveying, Mapping and Geoinformation, and the Chairperson of the Navigation and Location Service Session of China Satellite Navigation Conference. He has been engaged in the construction of the Beidou satellite navigation system and related scientific research work for a long time. His research interests include comprehensive PNT systems, integration of communication and navigation, and indoor positioning.

YACHUAN BAO received the B.E. and M.E. degrees from Xidian University, in 2009 and 2013, respectively, and the Ph.D. degree in engineering from the China Academic of Electronics and Information Technology, in 2017. He is currently a Senior Engineer with the State Key Laboratory of Satellite Navigation System and Equipment Technology, The 54th Research Institute of CETC. His research interests include satellite navigation, integrated communication and navigation, and indoor positioning. He is a member of the Indoor Navigation and Positioning Professional Committee of the China Satellite Navigation and Positioning Association and the Chinese Institute of Electronics and a Corporate Mentor with Xidian University and Zhejiang University.
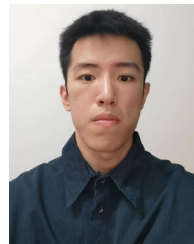
YUANKANG HUANG received the B.E. degree in communication engineering from the School of Electronics and Communication Engineering, Sun Yat-sen University (Shenzhen Campus), Shenzhen, China, in 2022, where he is currently pursuing the M.E. degree. His research interests include random access, the Internet of Things, and modeling of wireless networks.

WEN ZHAN (Member, IEEE) received the B.S. and M.S. degrees from the University of Electronic Science and Technology of China, China, in 2012 and 2015, respectively, and the Ph.D. degree from the City University of Hong Kong, China, in 2019. He was a Research Assistant and a Postdoctoral Fellow with the City University of Hong Kong. Since 2020, he has been with the School of Electronics and Communication Engineering, Sun Yat-sen University, China, where he is currently an Assistant Professor. His research interests include the Internet of Things, modeling, and performance optimization of next-generation mobile communication systems.

PEI LIU (Member, IEEE) received the B.E. degree in telecommunication engineering and the Ph.D. degree in information and communication engineering from the Huazhong University of Science and Technology (HUST), China, in 2014 and 2019, respectively. From 2016 to 2018, he held a joint Ph.D. Student and a Research Assistant with the Department of Electrical Engineering, City University of Hong Kong. In 2019, he joined the School of Information Engineering, Wuhan University of Technology, where he is currently an Assistant Professor and a Master's Supervisor. His research interests include massive MIMO, low-cost ADC, random access, and physical layer security.

• • •